2019 American Control Conference (ACC)
Philadelphia, PA, USA, July 10-12, 2019

Delay complementarity modeling for dynamic analysis of directional drilling

M.F. Shakib, E. Detournay, N. van de Wouw

***Abstract*— Hard-to-reach oil and gas reservoirs are nowadays accessed by directional drilling techniques, which use a rotary steerable system to drill complex curved boreholes. This paper aims at providing understanding of the complex behavior of directional drilling systems by developing a model for the borehole evolution and providing a dynamic analysis of the resulting model. The planar evolution of the borehole path is modeled in the form of a delay complementarity system, which accounts for undergauged stabilizers and a saturation of the bit orientation with respect to the borehole orientation. These are essential nonlinearities from a practical point of view. The pursued dynamic analysis reveals that these systems induce steady-state oscillations in the borehole path, which are related to the planar equivalent of the highly detrimental borehole spiraling observed in practice. The model and dynamic analysis provide essential insights and can serve in the further development of control techniques to track borehole paths while mitigating borehole spiraling.**

I. Introduction

Directional drilling allows for the drilling of boreholes with complex shapes, which are needed to access hard-to-reach reservoirs of oil, gas and mineral resources. A sketch of a directional drilling system is depicted in Figure 1. Such system includes a rig, which suspends the drillstring, a hollow slender tube that can be several kilometers in length. The rotary speed and the axial force (hook-load) are imposed at the rig. Most of the drillstring is in tension under its own weight, except for the bottom-hole assembly (BHA), which is in compression to induce a sufficient weight on bit. The BHA is usually in the order of ten meters long and consists of drill collars, three to five stabilizers to center the BHA in the borehole, a bit to drill the rock formation, various logging tools and a rotary steerable system (RSS). The RSS is a downhole robotic actuator that steers the bit in the desired direction. In this work, we consider the family of tools called push-the-bit RSS, which is located between the bit and the first stabilizer and uses a set of extensible pads to induce a lateral force on the side of the borehole and, thereby, on the BHA, which consequently steers the bit.

Borehole spiraling, being self-excited steady-state oscillations in the borehole path, is a well-known problem in directional drilling [2, 3]. An illustration of borehole spiraling is included in Figure 2, together with its two-dimensional equivalent called borehole rippling. Since the 1950's, many borehole propagation models [4]–[6], mostly numerical, have been developed to gain insight in the evolution of the borehole and/or to serve in the model-based control design for the RSS [7]. An advanced mathematical model is proposed in [8], which is able to determine conditions leading to unstable oscillatory behavior. This model has also been used to design controllers for the RSS to stabilize desired borehole trajectories [9, 10]. An extension of this model [1, 11] incorporates a saturation of the bit tilt, where the bit tilt is defined as the orientation difference between the bit and the borehole at the bit, see Figure 3. The saturation of the bit tilt is relevant from a practical point of view [12] since it occurs when the bit-gauge contacts a borehole wall. The bit tilt saturation boundary depends on the bit-gauge length and profile and is typically about 1° or less [1]. This nonlinearity prevents oscillations to grow unbounded and, consequently, these models capture borehole rippling and spiraling [11].

The aforementioned models do not consider stabilizers

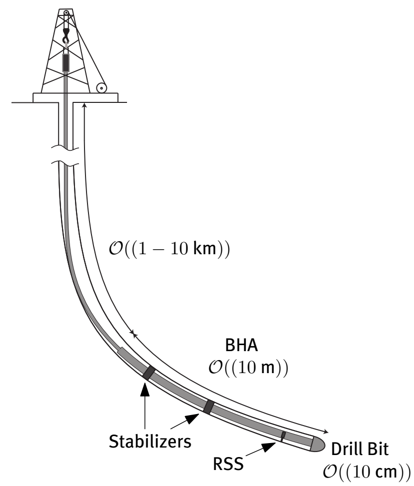

Fig. 1: Overview of a rotary directional drilling system [1].

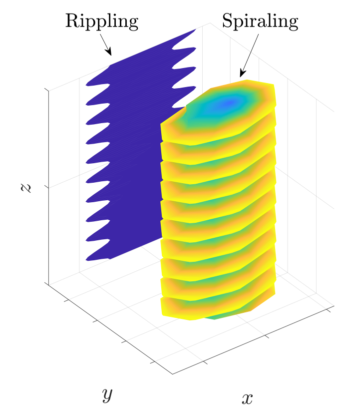

Fig. 2: Illustration of borehole spiraling and rippling.

M.F. Shakib is with the Department of Mechanical Engineering, Eindhoven University of Technology, Eindhoven, The Netherlands. m.f.shakib@tue.nl
E. Detournay is with the Department of Civil, Environmental, and Geo- Engineering, University of Minnesota, Minneapolis, USA. detou001@umn.edu
N. van de Wouw is with the Department of Mechanical Engineering, Eindhoven University of Technology, Eindhoven, The Netherlands. He is also with the Department of Civil, Environmental and Geo- Engineering, University of Minnesota, Minneapolis, USA. n.v.d.wouw@tue.nl

978-1-5386-7928-9/$31.00 ©2019 AACC

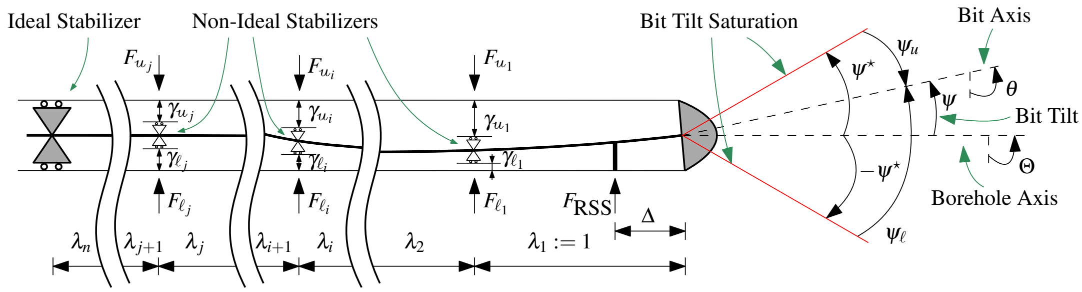

Fig. 3: Schematic overview of an n-stabilizer BHA. In this illustration, stabilizer j is perfectly centered inside the borehole such that $\gamma_{\ell_j} = \gamma_{u_j} = y^\star$.

that are undergauged with respect to the borehole, see Figure 3. Such stabilizers, defined as non-ideal stabilizers, are practically relevant due to a variety of reasons: (i) the design of undergauged stabilizers; (ii) a hole enlargement caused by erosion of the mud; and (iii) whirling of the bit/BHA. Typically, the clearance is of order $\mathcal{O}(1)$ cm [8].

In this paper, we develop a planar borehole propagation model as an extension of [1]. This model takes into account the bit tilt saturation and any number of non-ideal stabilizers in a framework based on linear complementarity problems, which yields a closed-form mathematical model description. Furthermore, we present a dynamic analysis of the resulting model that shows the central role of the nonlinearities in the so-called borehole rippling phenomenon.

II. Model Components

The model relies upon the following assumptions [1]:

1) The drilling process can be viewed as being rate-independent and, consequently, the independent variable is the borehole length measuring the arc-distance from the rig to the bit.
2) The drilling process can be averaged over several revolutions of the bit as fast dynamic processes are disregarded.
3) Only the lower part of the BHA, accounting for n stabilizers, needs to be study; the rest can be lumped into known forces acting on the last stabilizer, which is assumed ideal.
4) The BHA can be modeled statically as an Euler-Bernoulli beam with flexural stiffness EI.
5) There is no contact between the BHA and the borehole walls except for the bit, the pads of the RSS actuator and the stabilizers.

We present our model in dimensionless form where all forces are scaled with $F^\star := 3EI/\ell_1$ and all lengths are scaled with $\ell^\star := \ell_1$ with ℓ_1 the distance between the bit and the first stabilizer. The inclination of the borehole and bit are measured by the $\Theta(\xi)$ and $\theta(\xi)$, respectively, counter-clockwise with respect to the downward vertical direction, see Figure 3. These inclinations are tracked over the dimensionless borehole length ξ, which measures the increasing length of the borehole from the drill rig to the drill bit. Figure 4 depicts an overview of the model components and their interaction. These components are treated next.

A. Bit Kinematics

The bit kinematics describe the movement of the bit through the rock formation by an axial and lateral penetration variable d_1 and d_2, respectively, and an angular penetration variable φ. The bit tilt $\psi := \theta - \Theta$ can be expressed as

$$\psi = -\arctan\left(\frac{d_2}{d_1}\right) \approx -\frac{d_2}{d_1}, \tag{1}$$

since $d_1 \gg d_2$ because bits are designed to drill axially. The change of inclination of the bit with respect to the increasing borehole length can be characterized by

$$\frac{\mathrm{d}\theta}{\mathrm{d}\xi} \approx \frac{\varphi}{d_1}. \tag{2}$$

Equations (1) and (2) relate the bit motion to the penetration variables d_1, d_2 and φ and constitute the bit kinematics component of the model.

B. Bit-Rock Interaction

The bit-rock interaction can be expressed by the laws [13]:

$$N_0 = -G - H_1 d_1, \quad F_0 = -H_2 d_2, \quad M_0 = -H_3 \varphi, \tag{3}$$

where $G > 0$ is a measure of bit bluntness, N_0 and F_0 are the axial and lateral contact forces experienced by the bit, respectively, and M_0 is the contact moment acting on the bit (all dimensionless). Coefficients $H_i > 0$, for $i = 1,2,3$, relate the forces and moment acting on the bit to the penetration variables measuring the amount of rock removed by the bit in one revolution. With these definitions, the active weight on the bit can be defined as $\Pi := H_1 d_1 = -(N_0 + G)$. The active weight on bit is the part of the weight on the bit that is directly associated with the bit advancement into the rock.

The bit interface laws are formulated by combining the kinematic relations (1) and (2) with the bit-rock interaction laws (3)

$$F_0 = \eta \Pi (\theta - \Theta), \tag{4a}$$

$$M_0 = -\chi \Pi \frac{\mathrm{d}\theta}{\mathrm{d}\xi}, \tag{4b}$$

where $\eta := (H_2/H_1)$ and $\chi := (H_3/H_1)$ are the lateral and angular steering resistance, respectively. The parameter η takes a value between 5 and 100, while χ is generally one or two orders of magnitude smaller than η [13].

C. BHA Model

Using the Euler-Bernoulli beam theory, we statically fit the BHA, viewed as an elastic beam, inside the already drilled borehole geometry. Since we use the history of the borehole evolution, spatial delays, corresponding to the position of the stabilizers, arise naturally. A detailed derivation is given in [14], where we obtain analytical expressions for the scaled

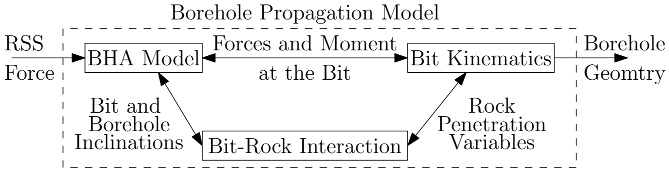

Fig. 4: Three model components and their interaction.

variables F_0, M_0 and the BHA deflection inside the borehole for any number of n stabilizers.

By combining the lateral force F_0 and the moment M_0 at the bit formulated in the BHA model with the relations found in the previous model components (4a) and (4b), the borehole propagation model is obtained. In these derivations, the forces experienced by the unilateral contact of the non-ideal stabilizers with the borehole walls and the bit tilt are treated as unknowns. These nonlinearities are modeled next.

III. Modeling of the Nonlinearities

The nonlinearities are modeled by formulating a linear complementarity problem (LCP). First the non-ideal stabilizers are treated. After that, the bit tilt saturation is addressed. Finally, an LCP that returns both the contact forces at the non-ideal stabilizers and the bit tilt, is formulated.

A. Non-Ideal Stabilizers

The BHA deflection, derived in the BHA model, with respect to the borehole center at stabilizer i is defined as δ_i. The variables δ_i are collected in the column δ, which can be written as

$$\delta = K^{-1}(F_\ell - F_u) + \tilde{q}(\langle\Theta\rangle_1, \dots, \langle\Theta\rangle_n, \theta, F_{\text{RSS}}), \tag{5}$$

where K and $\tilde{q}$ are given in (20) and (21) in the appendix. Variables F_ℓ and F_u are columns containing the contact forces F_{ℓ_i} and F_{u_i} experienced at each stabilizer as a result of contact with the lower and upper borehole walls, respectively, see Figure 3. The function $\tilde{q}$ depends on the applied RSS force F_{RSS}, the bit inclination θ and the average borehole inclinations $\langle\Theta\rangle_i$, for $i = 1, \dots, n$, defined as:

$$\langle\Theta\rangle_i(\xi) = \int_{s_{i-1}}^{s_i} \Theta(\xi - s)\,\mathrm{d}s \tag{6}$$

with s_i the distance from the bit to the i-th stabilizer. Next, Signorini's contact law [15] is employed for the unilateral contact between the non-ideal stabilizers and the (lower and upper) borehole walls:

$$\begin{aligned} &F_\ell \geq 0, \quad \gamma_\ell := y^\star + \delta \geq 0, \quad F_\ell^\top \gamma_\ell = 0, \\ &F_u \geq 0, \quad \gamma_u := y^\star - \delta \geq 0, \quad F_u^\top \gamma_u = 0. \end{aligned} \tag{7}$$

The variables γ_ℓ and γ_u are columns of gap variables γ_{ℓ_i} and γ_{u_i}, which measure the gap between stabilizer i and the lower and upper borehole wall, respectively, see Figure 3. Relations (7) follow from considering that the lower wall contact force F_{ℓ_i} can only be positive when stabilizer i contacts the lower wall, i.e., the gap $\gamma_{\ell_i} = 0$. On the other hand, when there is a positive gap $\gamma_{\ell_i} > 0$, the contact force $F_{\ell_i} = 0$. The same reasoning can be applied for upper wall contact. Parameters $y_i^\star$ are collected in $y^\star$ and represent the nominal clearance, i.e., the clearance when the stabilizer i is centered inside the borehole. The column vectors of gap variables are given by

$$\begin{aligned} \gamma_\ell &= K^{-1}(F_\ell - F_u) + \tilde{q} + y^\star, \\ \gamma_u &= K^{-1}(F_u - F_\ell) - \tilde{q} + y^\star, \end{aligned} \tag{8}$$

which are the linear equations required in the LCP formulated later.

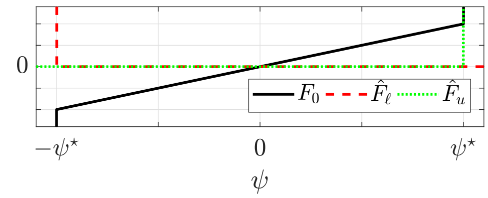

Fig. 5: Graphical interpretation of set-valued law (11).

B. Bit Tilt Saturation

Next, we will focus on the saturation of the bit tilt. First, we introduce parameter $\varepsilon := \chi/\eta$, such that the interface laws (4) contain only a product of η with Π:

$$F_0 = \eta\Pi(\theta - \Theta), \tag{9a}$$

$$M_0 = -\varepsilon\eta\Pi\frac{\mathrm{d}\theta}{\mathrm{d}\xi}. \tag{9b}$$

The parameter group $\eta\Pi$ has the interpretation of a pseudo-stiffness contrasting the flexural stiffness of the BHA with the penetration stiffness of the rock formation. Laboratory experiments [12, 16] show that the interface law (9a) is only valid for $|\psi| \leq \psi^\star$, where $\psi^\star$ is the saturation boundary. The lateral force at the bit F_0 is set-valued when the bit tilt saturates, i.e., $|\psi| = \psi^\star$. To model this nonlinearity, we measure the bit tilt from the lower and upper saturation boundary as follows:

$$\psi_\ell := \psi + \psi^\star, \tag{10a}$$

$$\psi_u := -\psi + \psi^\star, \tag{10b}$$

respectively. These variables are depicted in Figure 3 and can be interpreted as gap variables, similar to γ_ℓ and γ_u. The following set-valued force law [15] is introduced to characterize the bit tilt saturation:

$$\begin{aligned} &\hat{F}_\ell := -F_0 + \eta\Pi\psi \geq 0, \quad \psi_\ell \geq 0, \quad \hat{F}_\ell\psi_\ell = 0, \\ &\hat{F}_u := F_0 - \eta\Pi\psi \geq 0, \quad \psi_u \geq 0, \quad \hat{F}_u\psi_u = 0. \end{aligned} \tag{11}$$

Figure 5 provides a graphical interpretation of the force variables $\hat{F}_\ell$ and $\hat{F}_u$ as a function of the bit tilt ψ. From (11), we can observe the relation

$$\hat{F} := \hat{F}_\ell - \hat{F}_u = -2F_0 + 2\eta\Pi\psi, \tag{12}$$

which is used to write (10a) and (10b) as follows:

$$\begin{aligned} \psi_\ell &= \frac{1}{2\eta\Pi}\left(\hat{F}_\ell - \hat{F}_u\right) + \frac{F_0}{\eta\Pi} + \psi^\star, \\ \psi_u &= \frac{1}{2\eta\Pi}\left(\hat{F}_u - \hat{F}_\ell\right) - \frac{F_0}{\eta\Pi} + \psi^\star, \end{aligned} \tag{13}$$

where the lateral force at the bit is given by

$$F_0 = \sum_{i=1}^{n} a_i\left(\langle\Theta\rangle_i - \theta\right) + b\left(F_\ell - F_u\right) + c_1 F_{\text{RSS}} + c_2 \sin\langle\Theta\rangle_1 \tag{14}$$

with coefficients $a_1, \dots, a_n, b, c_1, c_2$ as in (24) in the appendix. Using (8), we eliminate F_ℓ and F_u in (14) and use the result in (13).

C. Combining both Nonlinearities

Considering the linear equations (8) and (13) and the complementarity relations (7) and (11), we arrive at the LCP

$$\underbrace{\begin{bmatrix} \gamma_\ell \\ \gamma_u \\ \psi_\ell \\ \psi_u \end{bmatrix}}_{w} = \underbrace{\begin{bmatrix} K^{-1} & -K^{-1} & 0 & 0 \\ -K^{-1} & K^{-1} & 0 & 0 \\ \frac{\mathscr{b}}{\eta\Pi} & -\frac{\mathscr{b}}{\eta\Pi} & \frac{1}{2\eta\Pi} & -\frac{1}{2\eta\Pi} \\ -\frac{\mathscr{b}}{\eta\Pi} & \frac{\mathscr{b}}{\eta\Pi} & -\frac{1}{2\eta\Pi} & \frac{1}{2\eta\Pi} \end{bmatrix}}_{M} \underbrace{\begin{bmatrix} F_\ell \\ F_u \\ \hat{F}_\ell \\ \hat{F}_u \end{bmatrix}}_{z} + \underbrace{\begin{bmatrix} \tilde{q}+y^\star \\ -\tilde{q}+y^\star \\ \hat{q}+\psi^\star \\ -\hat{q}+\psi^\star \end{bmatrix}}_{q}, \quad 0 \le w \perp z \ge 0, \tag{15}$$

where $K, \tilde{q}$ and $\hat{q}$ are given by (20) to (22) in the appendix, respectively. This LCP returns both the contact forces at the non-ideal stabilizers F_ℓ and F_u, together with their gap variables γ_ℓ and γ_u, as well as the bit tilt gap variables ψ_ℓ and ψ_u and the force variables $\hat{F}_\ell$ and $\hat{F}_u$. Once solved, the bit tilt can be calculated from the definition (10a) (or (10b)) and the lateral force at the bit F_0 can be retrieved via (12). The borehole inclination at the bit is simply given by

$$\Theta = \theta - \psi. \tag{16}$$

IV. Borehole Propagation Model

Combining expressions for M_0 from the interface law (9b) and from the BHA component results in the dynamics of θ:

$$\begin{aligned} \theta'(\xi) &:= \frac{\mathrm{d}\theta(\xi)}{\mathrm{d}\xi} = -\frac{M_0}{\varepsilon\eta\Pi} \\ &= \sum_{i=1}^{n} a_i\left(\langle\Theta\rangle_i - \theta\right) + b\left(F_\ell - F_u\right) + c_1\tilde{F}_{\mathrm{RSS}} + c_2 \sin\langle\Theta\rangle_1 \end{aligned} \tag{17}$$

with the coefficients $a_1,\ldots,a_n,b,c_1,c_2$ given in (23) in the appendix. The average borehole inclinations $\langle\Theta\rangle_i$, for $i = 1,\ldots,n$, defined in (6), are considered as additional state variables with dynamics

$$\langle\Theta\rangle_i'(\xi) := \frac{\mathrm{d}\langle\Theta\rangle_i(\xi)}{\mathrm{d}\xi} = \frac{\Theta_{i-1}-\Theta_i}{\lambda_i}, \tag{18}$$

where λ_i is the distance between the $(i-1)$-th and i-th stabilizer and Θ_i is a delayed version of the current borehole inclination defined as $\Theta_i := \Theta(\xi - s_i)$ with s_i the distance from the bit to the i-th stabilizer defined as $s_i := \sum_{k=0}^{i}\lambda_k$. The variables Θ_i represents the borehole inclination at stabilizer i. The output of the model is the borehole inclination $\Theta(\xi)$ calculated via (16).

The borehole propagation model consists of the set of delay differential equations (17) and (18), and the output equation (16), all subject to the LCP (15). This LCP returns the necessary contact forces F_ℓ and F_u experienced by the non-ideal stabilizers as well as the bit tilt ψ. The derived model is in the class of delay complementary systems [17], where the delayed geometric feedback of the borehole through the stabilizers is captured by the delayed borehole inclinations Θ_i in (18). The LCP framework is used to model the unilateral characteristics of the nonlinearities. These nonlinearities make the model exhibit many modes, which is captured in a compact model description using the LCP framework.

V. Stability Analysis

Borehole rippling is an expression of instability-induced steady-state oscillations in the borehole path. By performing a stability analysis, we aim to understand whether and under which conditions the developed model exhibits borehole rippling. In [17], conditions for the local and global asymptotic stability of equilibria of linear delay complementarity systems are proposed. Here we exploit these conditions for local asymptotic stability by linearizing the dynamics with respect to the considered borehole path and assessing stability of the linearized dynamics. We emphasize that this method is only valid as long as the borehole trajectory stays sufficiently close to the considered borehole path and the contact mode of the non-ideal stabilizers and the bit tilt mode remain unchanged locally around the considered borehole path. The dynamic behavior in which mode switching occurs is assessed through numerical simulations in Section VI.

To investigate the root cause of oscillatory behavior, it is sufficient to study the stability properties of straight borehole paths [14]. The linearized dynamics in state-space form examined near a straight borehole path read as

$$z'(\xi) = \sum_{i=0}^{n} \mathscr{A}_i^{(m)} z(\xi - s_i), \tag{19}$$

where z is the perturbed state, with respect to a nominal straight borehole path, $\mathscr{A}_i^{(m)}, i = 0,\ldots,n$, are system matrices and m is the considered mode. This linear DDE has the characteristic equation $\det\left(\nu I - \sum_{i=0}^{n}\mathscr{A}_i^{(m)} e^{-\nu s_i}\right) = 0$, which has an infinite number of roots ν_i with $i \in \{1,2,\ldots,\infty\}$ [18]. The roots of this characteristic equation represent the poles of (19). All these poles are located in the complex half plane characterized by $\mathscr{R}(\nu_i) < \upsilon$, where $\upsilon \in \mathbb{R}$ can be calculated numerically. The linearized dynamics in (19) are stable if and only if all the poles ν_i, for $i = 1,2,\ldots,\infty$, are located in the open complex left half plane (CLHP).

VI. Case Study

The method to assess stability described above is applied to a two-stabilizer model. This model accounts for a non-ideal stabilizer 3.66 m above the bit and an ideal stabilizer at 7.22 m above the bit, implying $\lambda_1 = \lambda_2 = 1$. The RSS actuator is placed 0.6 m above the bit. The BHA is characterized by a uniformly distributed weight of $1.08 \cdot 10^3$ N/m and a flexural stiffness of $7.2 \cdot 10^6$ Nm^2.

A key parameter in our model is $\eta\Pi$, which depends on the distance between the first stabilizer and the bit, the BHA stiffness, rock properties, bit design and active weight on the bit. Consequently, in practice, this parameter is often uncertain. Another important parameter is λ_2, which measures the dimensionless distance between the first and second stabilizer, see Figure 3. Since $\lambda_1 := 1$, representing the (dimensionless) distance between the bit and first stabilizer, λ_2 can be interpreted as the ratio between positions of the stabilizers. We assess stability for a grid of parameters $\eta\Pi$ and λ_2. A two-stabilizer model can exhibit four modes corresponding to the contact of the non-ideal stabilizer and the saturation of the bit tilt. Based on this distinction, Figure 6 presents a stability map in terms of the parameters $\eta\Pi$ and λ, where all the poles of (19) are in the open CLHP in the green areas, at least one real pole in the complex right half plane (CRHP) in the gray areas and at least one complex pole pair is in the CRHP in the red areas.

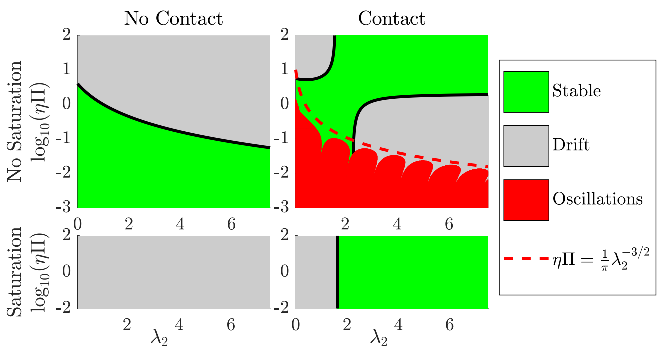

Fig. 6: Local stability of (19) for a grid of parameters $\eta\Pi$ and λ_2 for a two-stabilizer model. A distinction in the four subplots is made with respect to the active mode.

It can be observed in Figure 6 that in the mode where the non-ideal stabilizer contacts one of the walls and the bit tilt is not saturated, for some $\eta\Pi$, λ_2 settings, complex pole pairs are located in the CRHP, i.e., the red areas. This leads to an oscillatory growth of perturbations caused by the geometric feedback of the borehole sensed by the stabilizers and amplified at the bit. However, in other modes, for the exact same parametric setting, oscillatory instability does not occur, and instead stable behavior or a drift instability is observed. Steady-state borehole rippling is a consequence of the switching between such stable and unstable dynamics. Indeed, when a drilling system exhibits borehole rippling, the mode will change due to the saturation of the bit tilt and the contact of the non-ideal stabilizers. Thus the imposed nonlinearities are crucial for capturing steady-state borehole rippling oscillations. For the considered model, oscillatory behavior can be expected for $\eta\Pi < \eta\Pi|_s = 0.147$.

We illustrate our results with a simulation study, where we numerically integrate θ' in (17), and $\langle\Theta\rangle_i'$, for $i = 1,\dots n$, in (18), with respect to the independent variable ξ. The borehole inclination at the bit Θ is calculated via (16), stored and delayed to serve in the expressions for the delayed terms in $\langle\Theta\rangle_i'$ in (18). Furthermore, the LCP in (15) is solved during the simulation to update the contact forces and the bit tilt.

The simulations presented in Figures 7 and 8 are performed with $\eta\Pi = 0.01 < \eta\Pi|_s = 0.147$ and for a zero RSS actuation. An almost vertical downward borehole is taken as initial condition. For a stable system, the response should converge to a straight vertical borehole, i.e., $\Theta = 0$. First, in Figure 7, we present simulations with different bit tilt saturation boundaries $\psi^\star \in \{2°, 1°, 0.5°, 0.1°\}$ to show the effect of this nonlinearity on the obtained results. After that, the effect of the nominal clearance of the non-ideal stabilizer is addressed in Figure 8 by taking $y^\star \in \{1, 1.5, 2\} \cdot 10^{-3}$.

In Figure 7, it can be observed that all responses, except the one with $\psi^\star = 0.1°$, oscillate around the $\Theta = 0$. During one period, the bit tilt saturates on both sides and the non-ideal stabilizer contacts on both walls. Our stability analysis revealed that in case the bit tilt is not saturated, oscillatory behavior is induced when the non-ideal stabilizer contacts a wall. However, in all other modes the response should not oscillate. In particular, when the non-ideal stabilizer loses contact and the bit tilt does not saturate, the response is stable. Taking $\psi^\star$ sufficiently small, such as $\psi^\star = 0.1°$, generates a stable response. In general, a smaller $\psi^\star$ results in smaller oscillations in the bit and borehole inclinations and smaller contact forces experienced by the non-ideal stabilizer. This is expected as the BHA deforms less inside the borehole

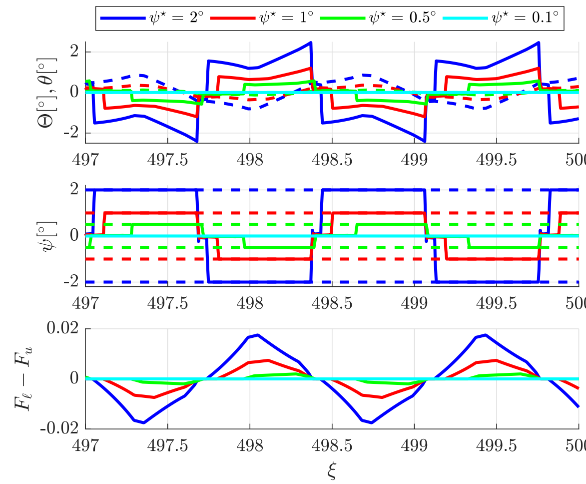

Fig. 7: Simulation results with $\eta\Pi = 0.01$ and bit tilt saturation boundaries $\psi^\star = \{2°, 1°, 0.5°, 0.1°\}$ and $y^\star = 0.001$.

for the bit tilt to reach the saturation boundary.

Figure 8 depicts the results of simulations with different nominal clearances $y^\star$ between the non-ideal stabilizer and the borehole walls. This clearance being small requires a small BHA deflection for the non-ideal stabilizer to contact with the borehole walls and, therefore, makes the response more prone to oscillatory behavior for such small $\eta\Pi$ setting. Increasing the clearance gives the non-ideal stabilizer more room to move and, hence, being cleared from both walls. In that case, the BHA acts as if equipped with only one stabilizer. Such BHAs do not generate oscillatory responses [1]. For a sufficiently large $y^\star$, the response thus remains stable. Generally, allowing for a larger clearance makes the response less prone to oscillatory behavior.

In field data displaying borehole spiraling [5, 11], it is observed that the oscillation wavelength is related to the distance between the bit and the first contact point of the drillstring with the borehole walls. In the simulations shown above in Figure 7 and Figure 8, the wavelength is approximately 1.3 in dimensionless length, which we can relate to the dimensionless distance between the bit and the non-ideal stabilizer defined as 1. Furthermore, in field data, the oscillation amplitude is of order $\mathcal{O}(10^{-3} \sim 10^{-2})$ m [5, 19], which also corresponds to our numerical results. Based on this comparison, we relate our results to borehole rippling, which is the two-dimensional equivalent of the harmful borehole spiraling observed in practice.

VII. Conclusions

This paper has presented a dynamic non-smooth borehole propagation model in the form of a delay complementarity system. The delay nature is a consequence of the delayed geometrical feedback of the borehole on the deformation of the drillstring through the stabilizers. A linear complementarity problem (LCP) framework is used to model two essential nonlinearities: the saturation of the bit tilt and any number of non-ideal stabilizers inducing unilateral contact. The LCP framework enables a compact formulation of the model, despite the large number of modes corresponding to the contact mode of the non-ideal stabilizers and the saturation mode of the bit tilt.

The local stability of equilibrium solutions in each mode has been assessed using spectral methods for delay systems. Our study revealed that in some modes, the system exhibits

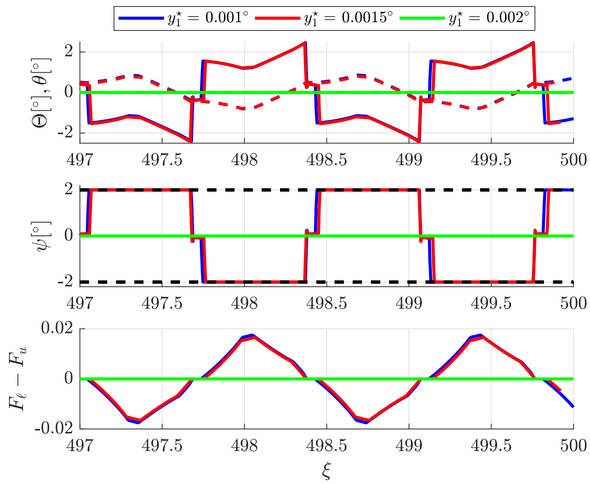

Fig. 8: Simulation results with $\eta\Pi = 0.01$ and different nominal clearances $y^\star = \{1, 1.5, 2\} \cdot 10^{-3}$ and $\psi^\star = 2°$.

an oscillatory-type of instability, while in other modes, the system is stable. The combination of such stable and unstable dynamics results in steady-state oscillations in the borehole, which represent borehole rippling.

The work presented in this paper provides insights in the behavior of directional drilling systems. The presented results can be used to improve directional drilling system design and form the basis for further work on control techniques to track predefined borehole paths while mitigating borehole rippling.

APPENDIX

The coefficients used in (17) and (14) are given in (23) and (24), respectively, where λ_i is the distance from stabilizer $i-1$ to stabilizer i, $s_i := \sum_{k=1}^{i} \lambda_k$ is the distance from the bit to the i-th stabilizer, $\lambda := s_n$ is the distance from the bit to the last stabilizer, Δ is the distance from the bit to the RSS and $\mathscr{w}$ is the distributed weight of the BHA. The row vectors b and $\mathscr{b}$ collect b_i and $\mathscr{b}_i$, for $i = 1, \ldots, n-1$, respectively. The i,j-th element of the matrix K^{-1} is given by

$$\begin{aligned} \left(K^{-1}\right)_{i,j} &= \sigma(s_i, s_j) \text{ for } i \geq j, \\ \left(K^{-1}\right)_{i,j} &= \sigma(s_j, s_i) \text{ for } i < j, \\ \sigma(s_i, s_j) &= \frac{s_i^2}{4\lambda^3}\left(s_j^2(3\lambda - s_j)(s_i - 3\lambda) + 2\lambda^3(3s_j - s_i)\right). \end{aligned} \tag{20}$$

Furthermore, the i-th row of $\tilde{q}$ is given by

$$\begin{aligned} \tilde{q}_i = &\sum_{k=1}^{i} \left(\lambda_{(k)}\left(\langle\Theta\rangle_k - \theta\right)\right) + \sum_{k=1}^{n} \left(\zeta_k(s_i)\left(\langle\Theta\rangle_k - \theta\right)\right) \\ &+ \zeta_{n+1}(s_i) F_{\mathrm{RSS}} + \zeta_{n+2}(s_i) \sin\langle\Theta\rangle_1 \end{aligned} \tag{21}$$

with functions

$$\begin{aligned} \zeta_k(s) &:= \frac{s^2(s-3\lambda)}{2\lambda^3}\lambda_k, \qquad \text{for } k = 1, 2, \ldots n, \\ \zeta_{n+1}(s) &:= \frac{\Delta^2}{4\lambda^3}(s^2(3\lambda - s)(\Delta - 3\lambda) + 2\lambda^3(3s - \Delta)), \\ \zeta_{n+2}(s) &:= \frac{1}{16}\tilde{\mathscr{w}} s^2(-3\lambda + 2s)(\lambda - s). \end{aligned}$$

Finally, the function $\hat{q}$ is given by

$$\hat{q} = \sum_{i=1}^{n} \frac{\mathscr{a}_i}{\eta\Pi}\left(\langle\Theta\rangle_i - \theta\right) + \frac{\mathscr{c}_1}{\eta\Pi}\tilde{F}_{\mathrm{RSS}} + \frac{\mathscr{c}_2}{\eta\Pi}\sin\langle\Theta\rangle_1 . \tag{22}$$

$$a_i = \frac{\lambda_{(i)}}{\varepsilon\eta\Pi\lambda^2} \tag{23a}$$

$$b_i = \frac{s_i(s_i - \lambda)(2\lambda - s_i)}{2\varepsilon\eta\Pi\lambda^2} \tag{23b}$$

$$c_1 = \frac{\Delta(\Delta - \lambda)(2\lambda - \Delta)}{2\varepsilon\eta\Pi\lambda^2} \tag{23c}$$

$$c_2 = \frac{1}{8\varepsilon\eta\Pi}\mathscr{w}\lambda^2 \tag{23d}$$

$$\mathscr{a}_i = \frac{\lambda_i}{\lambda^3} \tag{24a}$$

$$\mathscr{b}_i = \frac{2\lambda^3 - 3\lambda s_i^2 + s_i^3}{-2\lambda^3} \tag{24b}$$

$$\mathscr{c}_1 = \frac{\Delta^3 - 3\lambda\Delta^2 + 2\lambda^3}{-2\lambda^3} \tag{24c}$$

$$\mathscr{c}_2 = \frac{5}{8}\mathscr{w}\lambda \tag{24d}$$

REFERENCES

[1] L. Perneder, J. Marck, and E. Detournay, "A model of planar borehole propagation," *SIAM Journal on Applied Mathematics*, vol. 77, no. 4, pp. 1089–1114, 2017.

[2] G. Bellay, H. Al-Waheed, and T. Audah, "Cyclic borehole effects in deviated wells," in *Abu Dhabi International Petroleum Exhibition and Conference*, ser. Number SPE-36288-MS. Society of Petroleum Engineers, 1996, pp. 627–636.

[3] J. Sugiura and S. Jones, "Integrated approach to rotary-steerable drilling optimization using concurrent real-time measurement of near-bit borehole caliper and near-bit vibration," in *Intelligent Energy Conference and Exhibition*. Amsterdam, The Netherlands: Society of Petroleum Engineers, 2008, pp. 1–19.

[4] A. Lubinski and H.B. Woods, "Factors affecting the angle of Inclination and Dog-Legging in Rotary Bore Holes," in *Mid-Continent District*. Tulsa, Oklahoma, USA: American Petroleum Institute, 1953, pp. 222–250.

[5] P. Pastusek and V.J. Brackin, "A model for borehole oscillations," in *SPE Annual Technical Conference and Exhibition*. Denver, Colorado, USA: Society of Petroleum Engineers, 2003, pp. 1–16.

[6] G.C. Downton and M. Ignova, "Stability and response of closed loop directional drilling system using linear delay differential equations," in *Proceedings of the IEEE International Conference on Control Applications*, 2011, pp. 893–898.

[7] N. Panchal, M. Bayliss, and J. Whidborne, "Attitude control system for directional drilling bottom hole assemblies," *IET Control Theory and Applications*, vol. 6, no. 7, pp. 884–892, 2012.

[8] L. Perneder, "A three-dimensional mathematical model of directional drilling," Ph.D. dissertation, Faculty of the Graduate School of the University of Minnesota, Minneapolis, Minnesota, USA, 2013.

[9] N.A.H. Kremers, E. Detournay, and N. van de Wouw, "Model-based robust control of directional drilling systems," *IEEE Transactions on Control Systems Technology*, vol. 24, no. 1, pp. 226–239, 2016.

[10] O. Magana Villareal, E. Detournay, and N. van de Wouw, "Robust output-feedback control of 3D directional drilling systems," *International Journal of Robust and Nonlinear Control*, Accepted, 2018.

[11] J. Marck, E. Detournay, A. Kuesters, and J. Wingate, "Analysis of spiraled-borehole data by use of a novel directional-drilling model," *SPE Drilling and Completion*, vol. 29, pp. 267–278, March 2014.

[12] P.E. Pastusek, V.J. Brackin, and P.J. Lutes, "A fundamental model for prediction of hole curvature and build rates with steerable bottomhole assemblies," *SPE Annual Technical Conference and Exhibition*, pp. 1–7, 2005.

[13] L. Perneder, E. Detournay, and G. Downton, "Bit/rock interface laws in directional drilling," *International Journal of Rock Mechanics and Mining Sciences*, vol. 51, pp. 81–90, 2012.

[14] M.F. Shakib, "Nonlinear modeling for dynamic analysis of directional drilling processes," Master's thesis, Eindhoven University of Technology, Eindhoven, The Netherlands, 2017, D&C 2017.095.

[15] R. Leine and N. van de Wouw, *Stability and Convergence of Mechanical Systems with Unilateral Constraints*. Springer-Verlag Berlin Heidelberg, 2008, vol. 36.

[16] S. Ernst, P.E. Pastusek, and P.J. Lutes, "Effects of RPM and ROP on PDC Bit Steerability," in *SPE/IADC Drilling Conference*. Society of Petroleum Engineers, 2007.

[17] J.J.B. Biemond, W. Michiels, and N. van de Wouw, "Stability Analysis of Equilibria of Linear Delay Complementarity Systems," *IEEE Control Systems Letters*, vol. Vol. 1, no. 1, pp. 158–163, 2017.

[18] W. Michiels and S.J. Niculescu, *Stability and Stabilization of Time-Delay Systems: An Eigenvalue-Based Approach*. Philadelphia, USA: Society for Industrial and Applied Mathematics, 2007.

[19] F. E. Dupriest, W. C. Elks, S. Ottesen, P. E. Pastusek, J. R. Zook, and C. R. Aphale, "Borehole-Quality Design and Practices To Maximize Drill-Rate Performance," *SPE Drilling & Completion*, vol. 26, no. 02, pp. 303–316, 2011.